

# Magntohydrodynamic behavior of capacitor-coil target toward alternative inertial confinement fusion

T Sasaki<sup>1</sup>, S Oyama<sup>1</sup>, Y Sugimoto<sup>1</sup>, K Takahashi<sup>1</sup>, T Kikuchi<sup>1</sup>,  
N Harada<sup>1</sup>, H Nagatomo<sup>2</sup>, S Fujioka<sup>2</sup>, and A Sunahara<sup>3</sup>

<sup>1</sup>Nagaoka University of Technology, Nagaoka, Niigata, Japan

<sup>2</sup>Osaka University, Suita, Osaka, Japan

<sup>3</sup>Institute of Laser Technology, Osaka, Osaka, Japan

E-mail: [sasakit@vos.nagaokaut.ac.jp](mailto:sasakit@vos.nagaokaut.ac.jp)

**Abstract.** To understand its magnetohydrodynamic behaviors and the electrical properties, we proposed to evaluate both experimental observations and numerical simulations. Electrical conductivity for nickel in warm dense matter (WDM) state has been measured with an exploding wire in a quasi-isochoric vessel. The result shows that the electrical conductivity for nickel in WDM is relatively high from the comparison of the electrical conductivities for several materials in WDM state. However, the skin effect in the capacitor-coil target will be neglected from the estimation. A two-dimensional magnetohydrodynamic simulation for the capacitor-coil target has been demonstrated. The results shows that the distribution of B-field in the capacitor-coil target depends on the electrical conductivity model.

## 1. Introduction

Critical to fast ignition [1] is the transport of the laser-generated fast electrons and their associated heating of compressed DT fuel. The coupling efficiency of laser energy to these fast electrons and the energy deposited in the fuel should be improved by use of the guiding method [2, 3]. The fast electrons are transported with the strong magnetic field, which is order of several teslas, generated by a capacitor-coil target [4]. The capacitor-coil target as shown in Fig. 1 consists of two disks with a single-tune coil. When kJ and ns laser irradiates on the disk, the super-thermal hot electrons emits from the disk. The electrons as a current generates the strong magnetic field in the single tune coil. The generated magnetic field using capacitor-coil target depends on the coil materials [5, 6]. The generated magnetic field should be considered the generation rate of super-thermal hot electrons and the skin effect as an electrical conductivity for ablated plasma at the generation of the magnetic field. To understand its magnetohydrodynamic behaviors and the electrical properties, we proposed to evaluate experimental observations and numerical simulations.

To understand its magnetohydrodynamic behaviors and the electrical properties, we proposed to evaluate both experimental observations and numerical simulation. Electrical conductivity for nickel in warm dense matter (WDM) state has been measured with an exploding wire in a quasi-isochoric vessel. To understand the magnetohydrodynamic behavior in the capacitor-coil target, a two-dimensional MHD simulation has been also demonstrated.



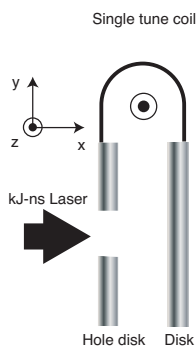


**Figure 1.** Image of capacitor-coil target.

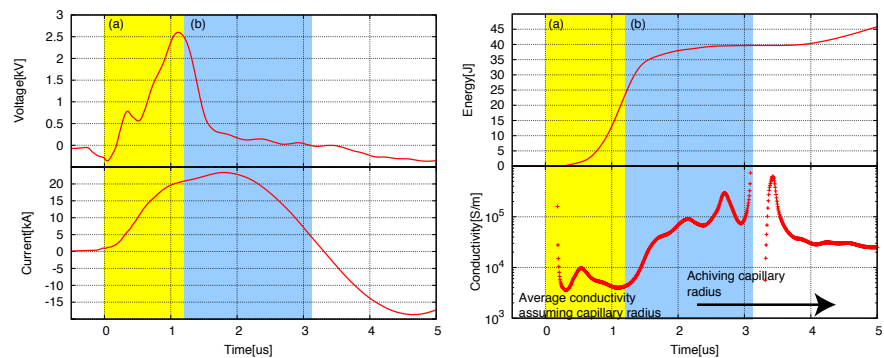


**Figure 2.** Time-evolution of exploding wire for nickel in the quasi-isochoric vessel. (1) voltage, (2) current, (3) input energy of the wire/plasma, and (4) electrical conductivity.

## 2. Evaluation of Electrical Conductivity using Exploding Wire Discharge with Isochoric Vessel

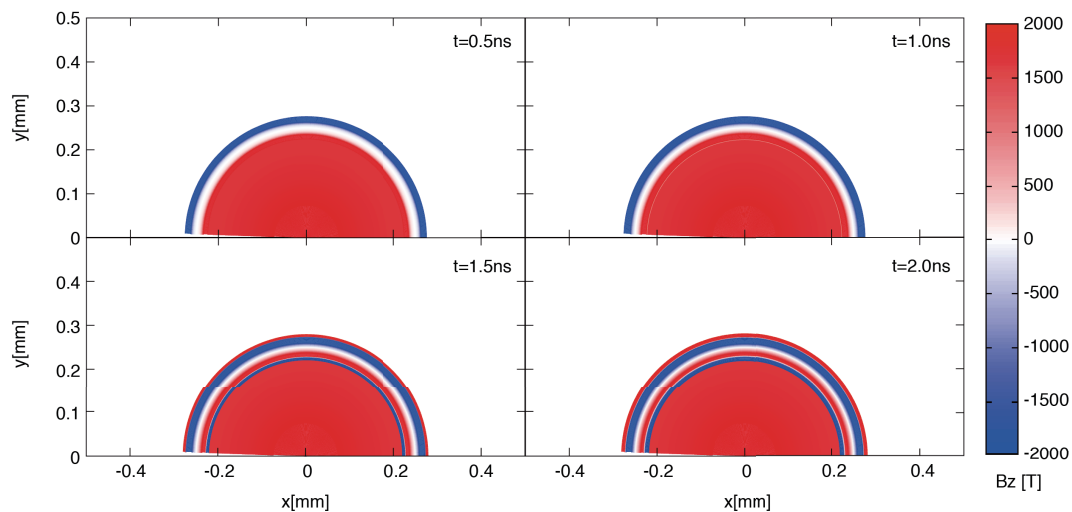
To observe the electrical conductivity in WDM, we have demonstrated an exploding wire discharge with quasi-isochoric vessel. The experimental setup of the exploding wire discharge with quasi-isochoric vessel as shown in Ref. [7]. A capacitor bank; C consists of  $2 \times 1.89 \mu\text{F}$  low-inductance capacitors, which drive a wire explosion. The capacitor bank was charged up to 8 kV, and it was switched by a low-inductance triggered spark gap. The wire/plasma was confined by the glass tube having  $\phi = 1$  mm in diameter with  $l = 10$  mm in length. The wire diameter was selected to be  $300 \mu\text{m}$ , considering the skin depth and the plasma density of the sample.

Figure 3 shows the typical voltage-current waveforms, input energy, and electrical conductivity of the sample. As shown in Fig. 3, the wire was exploded at  $1.2 \mu\text{s}$  from the voltage-current waveform. It means that the region (a) in Fig. 3 corresponds to the wire-vapor condition. After exploded wire, the wire-plasma expands in the isochoric vessel. The wire/plasma expansion velocity is estimated to be  $3 \times 10^3$  m/s from the optical emission of wire-plasma. The uniformity time of density distribution in the expanded wire plasma from exploding wire discharge in water is several hundreds ns, which depends on the sound velocity of the wire/plasma. Thus, the region (b) in Fig. 1 is the uniform wire/plasma state. After the region (b) in Fig. 3, the vessel was broken by the exploding wire/plasma. Observed electrical conductivity estimated by the plasma column size and voltage-current waveform is  $10^4 \sim 10^5$  S/m. Since the optical emission from wire/plasma is black-body, the wire/plasma temperature is estimated to be 5000 K.

From the comparison of the previous experimental results as shown in Ref. [8, 9, 10, 11], the electrical conductivities of the other materials are estimated to be  $10^4$  S/m at the same density-temperature. It means that the electrical conductivity of nickel is higher than that of the other materials at the same plasma density. From the measured electrical conductivities of several materials in WDM state, the skin depth  $\delta = \sqrt{1/\pi\mu_0 f\sigma}$ , where  $f$  is the typical frequency as 200 MHz, is larger than the wire diameter of the capacitor coil.

## 3. Magnetohydrodynamics Simulation on Capacitor-coil Target

To understand the dependence of generated magnetic field on electrical conductivity distribution in matter, the magnetohydrodynamics (MHD) of single tune coil in the capacitor-coil target with two-dimensional cylindrical geometry has been calculated. The simulation is not incorporated the experimental results. The MHD behavior of capacitor-coil target is solved by conventional



**Figure 3.** Time-evolutions of  $B_z$ -field profile in x-y plane, which is calculated using constant electrical conductivity for the wire.

MHD equations. The magnetic pressure in the equation of motion was neglected because the kinetic pressure of the plasma was higher than the magnetic pressure. The wire material, which is determine the equation of state and the transport properties, is aluminium. Coil and wire diameters of the capacitor-coil target at the initial condition were set to be  $550\ \mu\text{m}$  and  $50\ \mu\text{m}$ , respectively. The electrical conductivity in vacuum region is set to be  $10^{-5}\ \text{S/m}$ .

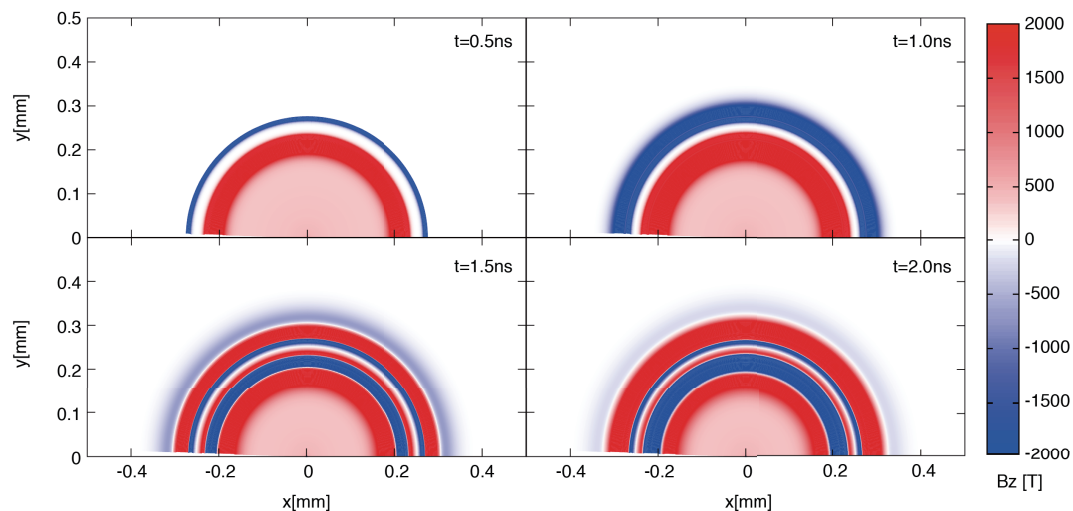
The capacitor-coil target during the irradiation of intense laser behaves like a current source. The maximum interior magnetic flux density of capacitor-coil coil is approximately 1.5 kT. From the results, to simplify the current evolution  $I(t)$ , we have set sinusoidal wave form with 4 MA of maximum current and 500 MHz of frequency. The displacement current was also neglected since the propagation time of the electromagnetic wave from the inner wire surface to the center of the coil was estimated to be 1 ps. The typical timescale of magnetohydrodynamic motion is longer than that of the electromagnetic wave. The timescale in the MHD simulation is ensured.

Figure 3 shows the time-evolutions of  $B_z$ -field profile, which is calculated using constant electrical conductivity for the wire. The electrical conductivity of wire is set to be  $10^5\ \text{S/m}$ . The results shows that  $B_z$ -field in the coil is almost uniform until  $t = 1\ \text{ns}$ . After  $t = 1\ \text{ns}$ , the isolated reversal  $B_z$ -field is observed. However, the  $B_z$ -field at the center of coil is positive until  $t = 2\ \text{ns}$ .

Figure 4 shows the time-evolutions of  $B_z$ -field profile, which is calculated using Lee-More model [12] for the wire. The results indicated that  $B_z$ -field in the coil using Lee-More model is rather small compared to that using constant conductivity model. Because the electrical conductivity of wire using Lee-More model is  $10^6\ \text{S/m}$ , the B-field diffuses into the coil. However, it is noted that the spatial-temporal distribution of B-field depends on the total current in the coil. Thus, the equivalent circuit model for capacitor-coil target or the total current into the coil will be included the simulation model.

#### 4. Concluding Remarks

To understand the magnetohydrodynamic behavior and electrical properties of the laser-capacitor target we have evaluated by experimental observations and numerical simulations. Electrical conductivity for nickel in WDM state has been measured with the exploding wire in the quasi-isochoric vessel. The result shows that the electrical conductivity for nickel in WDM



**Figure 4.** Time-evolutions of  $B_z$ -field profile in x-y plane, which is calculated using Lee-More model [12] for the wire.

is relatively high from the comparison of the electrical conductivities for several materials in WDM state. However, the skin effect in the capacitor-coil target will be neglected from the estimation. A two-dimensional magnetohydrodynamic simulation for capacitor-coil target has been demonstrated. The results shows that the distribution of B-field in the capacitor-coil target depends on the electrical conductivity model.

The equivalent circuit model for capacitor-coil target or the total current into the coil will be included the simulation model.

### Acknowledgements

This work was partly supported by the joint research project of the Institute of Laser Engineering, Osaka University (under contract subject "2015B1-13").

### References

- [1] Kodama R, *et al* 2001 *Nature* **412** 798
- [2] Kemp A J, Fiuza F, Debayle A, Johzaki T, Mori W, Patel P K, Sentoku Y and Silva L O 2014 *Nuclear Fusion* **54** 054002
- [3] Robinson A P L, *et al* 2014 *Nuclear Fusion* **54** 054003
- [4] Fujioka S, *et al* 2012 *Plasma Physics and Controlled Fusion* **54** 124042
- [5] Fujioka S, *et al* 2013 *Scientific Reports* **3** 1170
- [6] Santos J J, *et al* 2015 *New Journal of Physics* **17** 083051
- [7] Amano Y, *et al* 2012 *Review of Scientific Instruments* **83** 085107
- [8] Sasaki T, *et al* 2010 *Physics of Plasmas* **17** 084501
- [9] Sheftman D and Krasik Y E 2010 *Physics of Plasmas* **17** 112702
- [10] Sasaki T, *et al* 2006 *Laser and Particle Beams* **24** 371
- [11] Krisch I and Kunze H J 1998 *Physical Review E* **58** 6557
- [12] Lee Y T and More R M 1984 *Physics of Fluids* **27** 1273